

THE LATE-TIME REBRIGHTENING OF TYPE IA SN 2005GJ IN THE MID-INFRARED

ORI D. FOX^{1,2} & ALEXEI V. FILIPPENKO¹
Draft version November 22, 2018

ABSTRACT

A growing number of observations reveal a subset of Type Ia supernovae undergoing circumstellar interaction (SNe Ia-CSM). We present unpublished archival *Spitzer Space Telescope* data on SNe Ia-CSM 2002ic and 2005gj obtained > 1300 and 500 days post-discovery, respectively. Both SNe show evidence for late-time mid-infrared (mid-IR) emission from warm dust. The dust parameters are most consistent with a pre-existing dust shell that lies beyond the forward-shock radius, most likely radiatively heated by optical and X-ray emission continuously generated by late-time CSM interaction. In the case of SN 2005gj, the mid-IR luminosity more than doubles after 1 year post-discovery. While we are not aware of any late-time optical-wavelength observations at these epochs, we attribute this rebrightening to renewed shock interaction with a dense circumstellar shell.

Subject headings: circumstellar matter — supernovae: general — supernovae: individual (SN 2002ic, SN 2005gj) — dust, extinction — infrared: stars

1. INTRODUCTION

The ability to standardize Type Ia supernova (SN Ia) light curves yields precise cosmological distance indicators (e.g., Phillips 1993). Despite these empirical relationships, questions remain about the underlying physics and progenitor systems. The SN itself is generally accepted to be the thermonuclear explosion of a C/O white dwarf (WD), but the nature of the companion star remains ambiguous. Evidence now exists for both single-degenerate and double-degenerate (SD, DD) channels (e.g., Patat et al. 2007; Blondin et al. 2009; Simon et al. 2009; Nugent et al. 2011; Ganeshalingam et al. 2011; Brown et al. 2012; Foley et al. 2012a,b; Bloom et al. 2012; Silverman et al. 2012).

Recent studies reveal a subsample of SNe Ia that exhibit signs of significant interaction between the forward shock and a dense circumstellar medium (hereafter SNe Ia-CSM; Silverman et al. 2013b, and references within). The spectra show many similarities to those of SNe IIn, defined by their strong and relatively narrow hydrogen emission lines generated from a slow, dense, pre-existing CSM (Schlegel 1990; see Filippenko 1997 for a review). The SNe Ia-CSM also have slightly larger peak luminosities than typical SNe Ia, in the range $-21.3 \leq M_R \leq -19$ mag. Detailed observations of the nearby SN Ia-CSM PTF11kx confirm a probable SD channel for at least this particular event (Dilday et al. 2012; Silverman et al. 2013a).

Two of the most well-studied SNe Ia-CSM are 2002ic and 2005gj (Hamuy et al. 2003; Deng et al. 2004; Kotak et al. 2004; Wang et al. 2004; Wood-Vasey et al. 2004; Aldering et al. 2006; Prieto et al. 2007). The data suggest significant mass loss (of order $> 10^{-4} M_{\odot} \text{ yr}^{-1}$) from the companion star and significant amounts of warm dust emitting in the near-infrared (near-IR). These characteristics are also similar to those of SNe IIn. Owing to their dense CSM, SNe IIn exhibit late-time (> 100

day) IR emission from warm dust that is continuously heated by visible and X-ray radiation generated by ongoing CSM interaction (e.g., Gerardy et al. 2002; Fox et al. 2011). The CSM geometry derived from these dust shells reveals important clues about the progenitor mass-loss history.

In this *Letter* we present unpublished archival *Spitzer Space Telescope* data on SNe 2002ic and 2005gj obtained > 1300 and 500 days post-discovery, respectively. Section 2 lists the details of the observations; *Spitzer* photometry constrains the dust mass and temperature, and thus the luminosity. We explore the origin and heating mechanism of the dust in §3. §4 presents our conclusions.

2. OBSERVATIONS

2.1. Warm *Spitzer*/IRAC Photometry

A search in the *Spitzer* Heritage Archive (SHA)³ revealed unpublished observations of SNe 2002ic and 2005gj, summarized in Table 1. The SHA provide access to the Post Basic Calibrated Data (pbcd), which are already fully coadded and calibrated. Figure 1 shows false-color images of the combined 3.6 , 4.5 , and $5.8 \mu\text{m}$ channel images at a single epoch. The background flux in most of the SN host galaxies is bright and exhibits rapid spatial variations. Although template subtraction is a commonly used technique to minimize photometric confusion from the underlying galaxy, no pre-SN *Spitzer* observations exist. Instead, photometry was performed using the DAOPHOT aperture-photometry package (APPHOT) in IRAF.⁴ SN 2005gj falls $< 1''$ from the galactic nucleus (Aldering et al. 2006; Prieto et al. 2007). To minimize contributions from the underlying galaxy in both cases,

³ SHA can be accessed from <http://sha.ipac.caltech.edu/applications/Spitzer/SHA/>.

⁴ IRAF: the Image Reduction and Analysis Facility is distributed by the National Optical Astronomy Observatory, which is operated by the Association of Universities for Research in Astronomy (AURA) under cooperative agreement with the National Science Foundation (NSF).

¹ Department of Astronomy, University of California, Berkeley, CA 94720-3411.

² email: ofox@berkeley.edu .

Table 1
Spitzer Observations¹

SN	JD −2,450,000	Epoch (days)	PID	AOR	Distance (Mpc)	t_{int} (s)	$3.6 \mu\text{m}^3$	$4.5 \mu\text{m}^3$ ($10^{17} \text{ erg s}^{-1} \text{ cm}^{-2} \text{ \AA}^{-1}$)	$5.8 \mu\text{m}^3$	$8.0 \mu\text{m}^3$
2002ic	3386	795	3248	10550272	280	4000	0.150(0.075)	0.136(0.057)	0.092(0.038)	0.052(0.023)
2002ic	3770	1179	20256	14455040	280	3600	0.060(0.047)	0.063(0.039)	0.052(0.029)	0.040(0.020)
2002ic	3961	1370	30292	17965824	280	2400	0.042(0.039)	0.045(0.033)	0.037(0.024)	0.031(0.017)
2002ic	4356	1765	40619	23107840	280	2400	<0.03	<0.03	<0.03	<0.03
2005gj	3778	139	264	16868096	268	2400	0.130(0.069)	0.092(0.047)	0.036(0.024)	0.017(0.013)
2005gj	4004	365	30733	19308800	268	2400	0.183(0.082)	0.110(0.052)	0.049(0.028)	0.024(0.015)
2005gj	4149	510	30733	19309056	268	2400	0.276(0.101)	0.199(0.069)	0.113(0.043)	0.049(0.022)

¹ Upper limits for nondetections were derived by the point-source sensitivity in Table 2.10 of the IRAC Instrument Handbook, version 2.

² All distances are derived from the host-galaxy redshift assuming $H_0 = 72 \text{ km s}^{-1} \text{ Mpc}^{-1}$.

³ 1σ uncertainties are given in parentheses.

a 2-pixel radius was chosen and aperture corrections were applied, although removal of nuclear contributions is admittedly difficult.

2.2. Dust Temperature and Mass

Assuming only thermal emission, the mid-IR photometry provides a strong constraint on the dust temperature and mass, and thus the IR luminosity. For optically thin dust with mass M_d and particle radius a , at a distance d from the observer, thermally emitting at a single equilibrium temperature T_d , the flux can be written as (e.g., Hildebrand 1983)

$$F_\nu = \frac{M_d B_\nu(T_d) \kappa_\nu(a)}{d^2}, \quad (1)$$

where $B_\nu(T_d)$ is the Planck blackbody function and $\kappa_\nu(a)$ is the dust absorption coefficient.

For simple dust populations of a single size composed entirely of either silicates or graphite, the IDL MPFIT function (Markwardt 2009) finds the best fit (see Figure 2) of Equation 1 by varying M_d and T_d to minimize the value of χ^2 . The absorption coefficients, κ , are given in Figure 4 of Fox et al. (2010). We do not include the $8.0 \mu\text{m}$ data in our fits because of an apparent excess (see below). With only three data points at each epoch, we limit our fits to a single component (see Figure 2). Table 2 lists the best-fit parameters for graphite grains of size $a = 0.1 \mu\text{m}$ (standard grain parameters; see Fox et al. 2011).

2.3. Origin of the $8 \mu\text{m}$ Excess

There are several potential origins for the excess flux observed at $8.0 \mu\text{m}$ in Figure 2. (1) The $8.0 \mu\text{m}$ data may be the actual SN dust component, while the shorter wavelengths are dominated by an underlying galactic component. No single model, however, can reproduce the shorter-wavelength behavior in both SNe 2002ic and 2005gj. We therefore argue that the shorter-wavelength data are dominated by SN dust. (2) *Spitzer*'s Channel 4 bandpass extends out past $9.0 \mu\text{m}$, which includes the blue wing of a strong $10 \mu\text{m}$ feature associated with silicate dust grains (see Fox et al. 2010). We tried fitting silicate dust models to the *Spitzer* data in Figure 2, but find that the $8.0 \mu\text{m}$ data are not consistent with the expected intensity. We did not account for the Channel 4 filter transmission curve, but we do not expect this to have a large impact since the transmission remains fairly constant out past 9. We therefore rule out silicate dust, but note that it may contribute if a small fraction of the dust consists of silicates. (3) The $8.0 \mu\text{m}$ data may be caused by a second, colder SN dust component peaking at longer wavelengths. (4) The excess flux may be a result of a second, colder galactic dust component, but difficult to remove given the SN positions relative to their respective galactic nucleus and the poorer resolution at longer wavelengths. Because we lack longer-wavelength data, we cannot discriminate between these final two possibilities. Regardless of the origin, we exclude the $8.0 \mu\text{m}$ data from our fits.

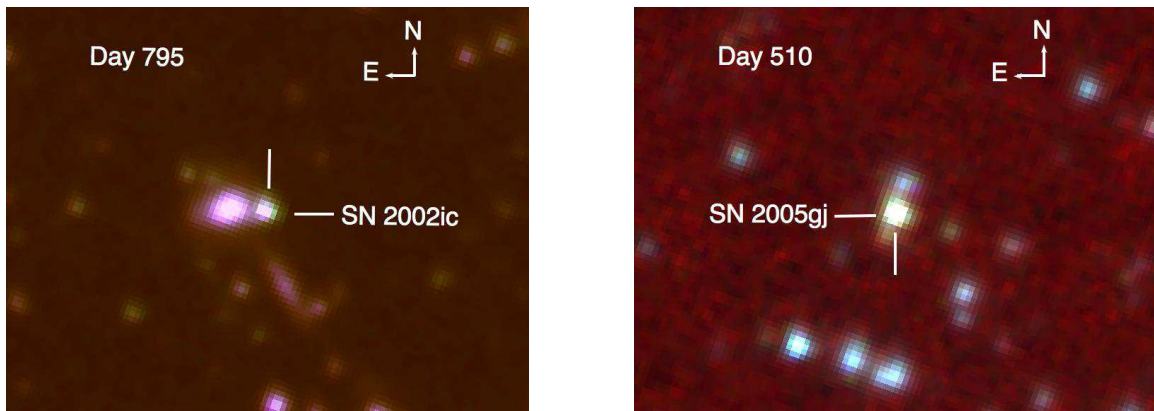


Figure 1. False-color 3.6, 4.5, $5.8 \mu\text{m}$ images of SNe 2002ic and 2005gj at late-times.

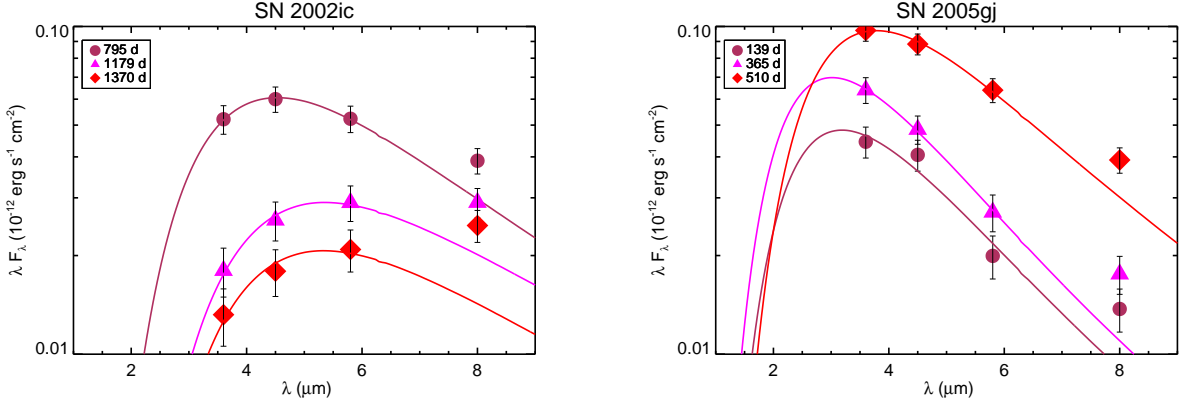


Figure 2. Photometry of SNe 2002ic and 2005gj in *Spitzer*/IRAC Channels 1 (3.6 μm), 2 (4.5 μm), 3 (5.8 μm), and 4 (8.0 μm). Overplotted are the resulting best fits of Equation 1.

3. ANALYSIS AND DISCUSSION

Figure 3 plots the corresponding IR luminosity evolution for each object. SN 2002ic remains bright ($L_d > 10^8 L_\odot$) for more than 2 yr post-discovery, but continues to fade throughout the observations. By contrast, SN 2005gj brightens after 1 year post-discovery. While we only have mid-IR photometry available at these epochs, we explore the constraints these data provide on the circumstellar environment.

3.1. Possible Origins and Heating Mechanisms

The source of the mid-IR emission is warm dust, but the origin and heating mechanism of the dust are less clear. The dust may be either newly formed or pre-existing, and either shock or radiatively heated; see Fox et al. (2010) for a full discussion. To discriminate between possible scenarios, we assume a spherically symmetric, optically thin dust shell and calculate the blackbody radius, $r_{\text{bb}} = [L_d/(4\pi\sigma T_d^4)]^{1/2}$, which sets a *minimum* shell size. A luminosity $L_d \approx 10^8 L_\odot$ and dust temperature $T_d \approx 500$ K yield a blackbody radius of $r_{\text{bb}} \approx 10^{17}$ cm. This radius is larger than that of a forward shock moving at $v_s \approx 10,000$ km s $^{-1}$ on day 800. This point seemingly rules out, particularly for SN 2005gj, the possibility of new dust formation in either the more slowly moving ejecta or the cold, dense shell (CDS) that can form behind the forward shock.

The alternative to newly formed dust is a pre-existing shell. Again, the fact that the blackbody radius is beyond the forward-shock radius rules out the likelihood of shock heating. Furthermore, an IR light-echo scenario (e.g., Dwek 1983), in which the dust shell is heated by the peak SN luminosity, is unfeasible. The implied shell radii ($r_{\text{echo}} = t_{\text{plateau}}/2c$) would require peak luminosities of nearly $10^{11} L_\odot$ to heat the dust to the observed temperatures.

In fact, the observed dust-shell parameters (i.e., radius, temperature, mass) are comparable to those seen in SNe IIn (e.g., Fox et al. 2011, 2013). In these cases, the pre-existing dust shell is continuously heated by optical and X-ray emission generated at inner radii by ongoing interaction between the forward shock and dense CSM. Assuming an optically thin dust shell, the observed dust temperature (\bar{T}_d) and shell radius (r_d) require a com-

bined optical, ultraviolet, and/or X-ray flux given by

$$L_{\text{opt/UV/X}} = \frac{64}{3} \rho a r_d^2 \sigma T_{\text{SN}}^4 \frac{\int B_\nu(T_d) \kappa(\nu) d\nu}{\int B_\nu(T_{\text{SN}}) Q_{\text{abs}}(\nu) d\nu} \quad (2)$$

for a dust bulk (volume) density ρ and an effective SN blackbody temperature T_{SN} , where B_ν is the Planck blackbody function, Q_{abs} is the dust absorption efficiency, and $\kappa(\nu)$ is the dust absorption coefficient. Figure 4 in Fox et al. (2013) shows that the blackbody radii of SNe 2002ic and 2005gj [$r_{\text{bb}} \approx (0.5\text{--}1.0) \times 10^{17}$ cm] at temperatures $T_d \approx 500\text{--}750$ K require optical and/or X-ray luminosities in the range $10^8 \lesssim L_{\text{opt/UV/X}} \lesssim 10^9 L_\odot$. While we don't have optical or X-ray observations at these epochs, the most recent optical observations of SNe 2002ic and 2005gj are consistent, with measured luminosities of $10^{9.1}$ and $10^{9.4} L_\odot$ on days 250 and 149, respectively (Deng et al. 2004; Prieto et al. 2007).

3.2. Evidence for Shells

Mid-IR wavelengths probe the characteristics of the CSM at the dust-shell radius. Assuming a dust-to-gas mass ratio expected in the H-rich envelope of a massive star, $Z_d = M_d/M_g \approx 0.01$, the dust-shell mass can be tied to the progenitor's total mass-loss rate,

$$\begin{aligned} \dot{M}_{\text{outer}} &= \frac{M_d}{Z_d \Delta r} v_w \\ &= \frac{3}{4} \left(\frac{M_d}{M_\odot} \right) \left(\frac{v_w}{120 \text{ km s}^{-1}} \right) \left(\frac{5 \times 10^{16} \text{ cm}}{r} \right) \left(\frac{r}{\Delta r} \right) M_\odot \text{ yr}^{-1} \end{aligned} \quad (3)$$

for a progenitor wind speed v_w . The relatively narrow lines observed in SNe Ia-CSM originate in the slow pre-shocked CSM and can be used to approximate the progenitor wind speed. The precursor wind velocities for SNe 2002ic and 2005gj are $v_w = 100$ and 60 km s $^{-1}$, respectively (Kotak et al. 2004; Aldering et al. 2006). Assuming a thin shell, $\Delta r/r = 1/10$, wind speed $v_w = 60$ km s $^{-1}$, and radius $r_{\text{bb}} = 10^{17}$ cm, the approximate mass-loss rate to produce the observed dust shell is $\dot{M}_{\text{outer}} \approx 10^{-2} M_\odot \text{ yr}^{-1}$. A smaller dust-shell radius would require an even larger mass-loss rate.

The optical and/or X-ray emission generated by CSM interaction traces the mass loss at the inner radii. Assuming a density $\propto r^{-2}$ wind profile, the rate can

Table 2
IR Fitting Parameters ($a = 0.1 \mu\text{m}$)

SN	Epoch (days)	M_d (M_\odot)	T_d (K)	L_d (L_\odot)
2002ic	795	0.019	554	1.54×10^8
2002ic	1179	0.019	489	7.58×10^7
2002ic	1370	0.013	488	5.38×10^7
2005gj	139	0.002	783	1.17×10^8
2005gj	365	0.002	805	1.61×10^8
2005gj	510	0.010	655	2.35×10^8

be written as a function of the optical/X-ray luminosity, progenitor wind speed, and shock velocity (e.g., Chugai & Danziger 1994; Smith et al. 2009):

$$\begin{aligned} \dot{M}_{\text{inner}} &= \frac{2v_w}{\epsilon v_s^3} L_{\text{opt/UV/X}}, \\ &= 2.1 \times 10^{-4} \left(\frac{L_{\text{opt/UV/X}}}{3 \times 10^{41} \text{ erg s}^{-1}} \right) \left(\frac{\epsilon}{0.5} \right)^{-1} \times \\ &\quad \left(\frac{v_w}{120 \text{ km s}^{-1}} \right) \left(\frac{v_s}{10^4 \text{ km s}^{-1}} \right)^{-3} M_\odot \text{ yr}^{-1}, \quad (4) \end{aligned}$$

where $\epsilon < 1$ is the efficiency of converting shock kinetic energy into visual light. While the conversion efficiency varies greatly depending on shock speed and wind density, we assume $\epsilon \approx 0.5$, acknowledging that this value may be too high. Again, we do not have late-time optical or X-ray observations, but we do have theoretical estimates from Equation 2 in §3.1. An optical luminosity $L_{\text{opt/UV/X}} \approx 10^{8.5} L_\odot$, wind speed $v_w = 120 \text{ km s}^{-1}$, shock velocity $v_s = 10,000 \text{ km s}^{-1}$ (Deng et al. 2004), and conversion efficiency $\epsilon = 0.1$ correspond to a mass-loss rate $\dot{M}_{\text{inner}} \approx 10^{-3} M_\odot \text{ yr}^{-1}$.

While the variables used above are only order-of-magnitude approximations, the derived rate for \dot{M}_{inner} reveals two things about the circumstellar medium. (1) The difference between the mass-loss rates ($\dot{M}_{\text{inner}} < \dot{M}_{\text{outer}}$) suggests that the dust shells were formed during a period of increased, nonsteady mass-loss. (2) Compared to mass-loss rates derived from optical data at earlier epochs, our estimate of $\dot{M}_{\text{inner}} \approx 10^{-3} M_\odot \text{ yr}^{-1}$ is consistent with SN 2002ic on day 250 (for $\epsilon \approx 0.1$; Kotak et al. 2004), but at least an order of magnitude larger than that measured for SN 2005gj on day 74 (Prieto et al. 2007). The increased circumstellar density derived for SN 2005gj at this late time suggests the presence of another shell of material.

The decline of SN 2002ic occurs at >800 days, corresponding to the time at which the forward shock ($v_s = 10,000 \text{ km s}^{-1}$) would reach the blackbody radius ($r_{\text{bb}} \approx 10^{17} \text{ cm}$). The declining light curve may be attributed to the forward shock overtaking and destroying the dust and/or a decreasing amount of CSM interaction accompanied by a declining radiative heating source.

Alternatively, the rebrightening of the pre-existing dust in SN 2005gj is likely due to radiative heating by renewed shock interaction with this dense circumstellar shell. From Equation 4, an order-of-magnitude increase in mass loss results in an increase in the optical luminosity by a factor of 3–4, assuming the shock velocity decreases to 0.8 of its former value. For a constant blackbody radius of $r_{\text{bb}} \approx 5 \times 10^{16} \text{ cm}$, Equation 2 and Figure

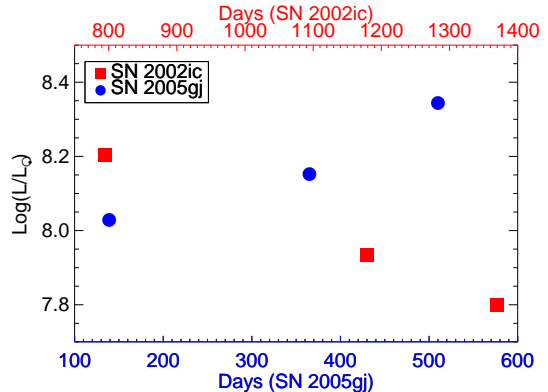


Figure 3. The late-time mid-IR luminosity evolution of SNe 2002ic and 2005gj. The luminosity is derived by summing over the modified blackbody fits given in Equation 1 and shown in Figure 2. SN 2005gj exhibits an unanticipated rise more than a year post-discovery, suggesting renewed shock interaction between the forward shock and a pre-existing circumstellar shell.

10 in Fox et al. (2010) show that an increase in the optical luminosity from 10^8 to $10^{8.4} L_\odot$ results in a dust temperature increase from ~ 600 to 750 K . Since $L_d \propto T_d^4$, this change in temperature results in a luminosity increase of a factor of 2.4.

While we observe a luminosity increase of this magnitude (see Table 2), the inferred dust temperature actually *decreases* by $\sim 150 \text{ K}$. The implication is that the blackbody radius must also increase from 5×10^{16} to 10^{17} cm , which would explain a lower dust temperature along with a higher dust mass and luminosity. The problem with invoking this scenario is that the only way to increase the blackbody radius (assuming a spherically symmetric shell of dust) would be for the increased optical luminosity to vaporize all dust out to the new blackbody radius. For a dust vaporization temperature of $T_{\text{evap}} \approx 2000 \text{ K}$, Equation 2 and Figure 8 in Fox et al. (2010) show that to vaporize dust out to 10^{17} cm requires a luminosity of $> 10^{10} L_\odot$, which is not likely. The more probable explanation is that with only three data points, the slopes of the curves in Figure 2 and, therefore the temperatures, are biased by contamination from the underlying galaxy nucleus ($< 1''$ away and a $0.6''$ pixel scale). The total dust luminosity, which is less sensitive to the slope, is most consistent with radiative heating by renewed shock interaction.

4. SUMMARY

This letter presents unpublished archival *Spitzer* data on SNe Ia-CSM 2002ic and 2005gj obtained > 1300 and 500 days post-discovery. The mid-IR data show evidence of emission from warm dust. While we don't have simultaneous observations at shorter wavelengths, the warm dust parameters are most constant with a pre-existing dust shell heated by a combination of optical, UV, and X-ray emission continuously generated by ongoing CSM interaction. The degree of CSM interaction dictates the dust temperature and, thereby, the luminosity. In the case of SN 2005gj, the mid-IR luminosity nearly doubles more than 1 year post-discovery, suggesting an increasing amount of CSM interaction. We attribute this renewed shock interaction to a dense circumstellar shell produced during a period of increased mass loss by

the progenitor companion. While progenitor mass-loss provides additional support for a SD channel, future multi-wavelength observations of SNe Ia-CSM will be necessary to better trace the complete mass-loss history and constrain the nature of the companion star.

This work is based on archival data obtained with the *Spitzer Space Telescope*, which is operated by the Jet Propulsion Laboratory, California Institute of Technology, under a contract with NASA. Support for this work was provided by NASA through an award issued by JPL/Caltech (P90031). A.V.F. and his group acknowledge generous financial assistance from the Richard and Rhoda Goldman Fund, the Christopher R. Redlich Fund, the TABASGO Foundation, and NSF grant AST-1211916.

REFERENCES

- Aldering, G., et al. 2006, *ApJ*, 650, 510
 Blondin, S., Prieto, J. L., Patat, F., Challis, P., Hicken, M., Kirshner, R. P., Matheson, T., & Modjaz, M. 2009, *ApJ*, 693, 207
 Bloom, J. S., et al. 2012, *ApJL*, 744, L17
 Brown, P. J., Dawson, K. S., Harris, D. W., Olmstead, M., Milne, P., & Roming, P. W. A. 2012, *ApJ*, 749, 18
 Chugai, N. N., & Danziger, I. J. 1994, *MNRAS*, 268, 173
 Deng, J., et al. 2004, *ApJ*, 605, L37
 Dilday, B., et al. 2012, *Science*, 337, 942
 Dwek, E. 1983, *ApJ*, 274, 175
 Filippenko, A. V. 1997, *ARA&A*, 35, 309
 Foley, R. J., et al. 2012a, *ApJ*, 752, 101
 —. 2012b, *ApJ*, 744, 38
 Fox, O. D., Chevalier, R. A., Dwek, E., Skrutskie, M. F., Sugerman, B. E. K., & Leisenring, J. M. 2010, *ApJ*, 725, 1768
 Fox, O. D., Filippenko, A. V., Skrutskie, M. F., Silverman, J. M., Ganeshalingam, M., Cenko, S. B., & Clubb, K. I. 2013, arXiv:1304.0248
 Fox, O. D., et al. 2011, *ApJ*, 741, 7
 Ganeshalingam, M., Li, W., & Filippenko, A. V. 2011, *MNRAS*, 416, 2607
 Gerardy, C. L., et al. 2002, *ApJ*, 575, 1007
 Hamuy, M., et al. 2003, *Nature*, 424, 651
 Hildebrand, R. H. 1983, *QJRAS*, 24, 267
 Kotak, R., Meikle, W. P. S., Adamson, A., & Leggett, S. K. 2004, *MNRAS*, 354, L13
 Markwardt, C. B. 2009, in *Astronomical Data Analysis Software and Systems XVIII*, ed. D. A. Bohlender, D. Durand, & P. Dowler (San Francisco: ASP), 251
 Nugent, P. E., et al. 2011, *Nature*, 480, 344
 Patat, F., et al. 2007, *Science*, 317, 924
 Phillips, M. M. 1993, *ApJ*, 413, L105
 Prieto, J. L., et al. 2007, arXiv:0706.4088
 Schlegel, E. M. 1990, *MNRAS*, 244, 269
 Silverman, J. M., et al. 2012, *MNRAS*, 425, 1789
 —. 2013a, arXiv:1303.7234
 —. 2013b, arXiv:1304.0763
 Simon, J. D., et al. 2009, *ApJ*, 702, 1157
 Smith, N., et al. 2009, *ApJ*, 695, 1334
 Wang, L., Baade, D., Höflich, P., Wheeler, J. C., Kawabata, K., & Nomoto, K. 2004, *ApJ*, 604, L53
 Wood-Vasey, W. M., Wang, L., & Aldering, G. 2004, *ApJ*, 616, 339